PHYSICAL REVIEW A VOLUME 15, NUMBER 1 JANUARY 1977

Elastic scattering of electrons and positrons by complex atoms at intermediate energies*

F. W. Byron, Jr.
Department of Physics and Astronomy, University of Massachusetts, Amherst, Massachusetts 01002

Charles J. Joachain
Physique Théorique, Faculté des Sciences, Université Libre de Bruxelles, Brussels, Belgium and Institut de Physique Corpusculaire, Université de Louvain, Louvain-la-Neuve, Belgium
(Received 13 January 1975; revised manuscript received 14 July 1975)

The elastic scattering of fast electrons and positrons by complex atoms is analyzed by using the basic ideas of the eikonal-Born series method within the framework of the optical-model formalism. This approach allows us to derive from first principles a local second-order pseudopotential which in addition to the static interaction also accounts for polarization, absorption, and exchange effects. A full wave treatment of this pseudopotential is then performed. Our *ab initio* optical-model theory is illustrated by a detailed analysis of the elastic scattering of electrons and positrons by helium and neon atoms for incident energies ranging from 100 to 700 eV. Our theoretical values for electron-helium and electron-neon differential cross sections are in excellent agreement with recent absolute experimental data.

I. INTRODUCTION

We have recently proposed a new approach—the eikonal-Born series (EBS) method—for analyzing the elastic scattering of electrons or positrons by atoms at intermediate and high energies.[1-3] This method, which gives a consistent picture of the differential cross section through order k^{-2} (where k is the incident-particle wave number), has been applied successfully to the analysis of the elastic scattering of fast electrons and positrons by atomic hydrogen[1,3] and helium.[1,2]

Since the calculation of the EBS scattering amplitude involves the evaluation of such quantities as the second term of the Born series (by using closure methods), it is clear that in practice the range of application of the EBS method is restricted to relatively simple atoms. Thus, in order to analyze the elastic scattering of electrons or positrons by complex atoms, other approaches are needed, which lead to tractable computational schemes. One of these approaches is the optical-model formalism[4-7] which has attracted considerable interest in recent years.[8-20] In this paper, we show that it is possible to use the basic ideas of the EBS method within the framework of the optical-model formalism to perform *ab initio* optical-model calculations of elastic electron- or positron-atom scattering. Our approach, which is based on a multiple scattering expansion[21] of the optical potential in terms of the full interaction between the incident particle and the target atom, applies essentially to the region of intermediate and high energies. It consists basically of constructing a local, second-order pseudopotential which is derived from first principles. In addition to the *static* interaction, this potential also accounts for dynamic *polarization* and *absorption* effects (obtained by using the properties of the EBS method) together with exchange effects. The only parameter in our theory is an average target excitation energy Δ, which we determine by requiring that the long-range form of the polarization potential be $-\bar{\alpha}/(2r^4)$, where $\bar{\alpha}$ is the dipole polarizability of the target atom.[22] In contrast with recent eikonal optical-model calculations,[13,14,18] we have used here the partial wave method to perform a full wave treatment of the optical potential. In this way, we are able to avoid certain difficulties associated with the use of the eikonal approximation.[18] A preliminary version of the present work has been given elsewhere.[19,20]

We begin in Sec. II by presenting our approach to the determination of the optical potential from first principles. In Sec. III, we apply this *ab initio* optical-model theory to study elastic scattering of fast electrons and positrons by helium. This is an important test case, for which we are able to compare our theoretical results with ones we have previously obtained from the EBS method,[1,2] as well as with recent absolute measurements of differential cross sections for incident electrons.[23-28] We find that the agreement between theory and experiment is excellent. We also discuss total cross sections and compare our calculations with the experimental data which have been obtained both for electron-helium[28-31] and positron-helium[32-35] scattering.

Section IV is devoted to a detailed analysis of the elastic scattering of fast electrons and positrons by neon, a problem on which little theoretical work has been done so far.[17,36-39] Our results for elastic electron-neon differential cross sections agree well with the recent absolute experimental data[26,28,40] above incident-electron energies of 200 eV, particularly in the small-angle region where the scattering is very large. We also discuss total cross sections for electron-neon scattering.[28,30,41] Finally, we consider positron-neon scattering and compare our total-cross-section values with recent experimental data.[32,42]

II. THEORY

Let us consider the nonrelativistic elastic scattering of an electron or a positron by a neutral atom of atomic number Z. We denote by $\mathcal{K}$ the kinetic-energy operator of the projectile, while h is the internal target Hamiltonian having eigenkets $|n\rangle$ and eigenenergies ω_n; we use the symbols $|0\rangle$ and ω_0 to denote, respectively, the ground-state eigenket and eigenenergy of the target atom. The free motion of the system before the collision is described by the Hamiltonian $H_0 = \mathcal{K}+h$. The full Hamiltonian of the system is given by $H=H_0+V$, where

$$V(\vec{r},X)=\frac{ZQ}{r}-Q\sum_{i=1}^{Z}\frac{1}{|\vec{r}_i-\vec{r}|} \tag{2.1}$$

is the interaction potential between the projectile and the target, with $Q=+1$ for incident positrons and $Q=-1$ for incident electrons. The symbol X denotes all the target coordinates.

We now write the equivalent one-body Schrödinger equation for elastic scattering, namely,

$$[\mathcal{K}+\mathcal{V}_{\text{opt}}-\tfrac{1}{2}k^2]\psi_i^{(+)}=0\ , \tag{2.2}$$

where $\psi_i^{(+)}$ is the elastic scattering wave function describing the motion of the projectile in the optical potential $\mathcal{V}_{\text{opt}}$. We shall first consider *direct* elastic scattering; exchange effects which occur when the incident particle is an electron will be discussed at the end of this section. Calling V_{opt}^d the part of the optical potential which governs direct scattering, we write V_{opt}^d to second order in a multiple scattering expansion (in terms of the full interaction V) as

$$V_{\text{opt}}^d=V^{(1)}+V^{(2)}\ . \tag{2.3}$$

Here the first order or static potential is given by

$$V^{(1)}=V_{\text{st}}=\langle 0|V|0\rangle\ , \tag{2.4}$$

while the second-order part $V^{(2)}$ reads

$$V^{(2)}=\sum_{n\neq 0}\frac{\langle 0|V|n\rangle\langle n|V|0\rangle}{\frac{1}{2}k^2-\mathcal{K}-(\omega_n-\omega_0)+i\epsilon}\ ,\quad \epsilon\to 0^+\ . \tag{2.5}$$

The summation in Eq. (2.5) runs over all the target states, except the ground state.

Since we are dealing with the region of intermediate and high energies we shall replace the differences $\omega_n-\omega_0$ in Eq. (2.5) by an average excitation energy Δ. Performing the summation on n in Eq. (2.5) by closure, we then obtain for $V^{(2)}$ in the coordinate representation the nonlocal, complex expression

$$\langle\vec{r}\,|V^{(2)}|\,\vec{r}'\rangle=G_0^{(+)}(k',\vec{r},\vec{r}')A(\vec{r},\vec{r}')\ , \tag{2.6}$$

where

$$G_0^{(+)}(k',\vec{r},\vec{r}')=-(2\pi)^{-3}\lim_{\epsilon\to 0^+}\int\frac{e^{i\vec{p}\cdot(\vec{r}-\vec{r}')}}{p^2/2-k'^2/2-i\epsilon}\,d\vec{p} \tag{2.7}$$

is the single-particle free propagator corresponding to the wave number

$$k'=(k^2-2\Delta)^{1/2}\ , \tag{2.8}$$

and

$$A(\vec{r},\vec{r}')=\langle 0|V(\vec{r},X)V(\vec{r}',X)|0\rangle - \langle 0|V(\vec{r},X)|0\rangle\langle 0|V(\vec{r}',X)|0\rangle\ . \tag{2.9}$$

The Schrödinger equation (2.2) then reads

$$[-\tfrac{1}{2}\nabla_{\vec{r}}^{\,2}+V_{\text{st}}(\vec{r})-\tfrac{1}{2}k^2]\psi_i^{(+)}(\vec{r}) + \int G_0^{(+)}(k',\vec{r},\vec{r}')A(\vec{r},\vec{r}')\psi_i^{(+)}(\vec{r}')\,d\vec{r}'=0\ . \tag{2.10}$$

This equation is still difficult to solve because of the nonlocal character of $V^{(2)}$. Previous studies of Eq. (2.10), carried out within the framework of the eikonal approximation,[13,14,18] showed how absorption[13,14] and polarization[18] effects can be taken into account for small-angle scattering. However, for large-angle electron- (positron-) atom elastic scattering eikonal methods may lead to serious inaccuracies in the intermediate-energy region. The main reason for this is *not* the inability of eikonal methods to handle large-angle scattering by long-range forces,[43] since the large-angle electron- (positron-) atom elastic scattering is dominated by the short-range static potential.[1-3] The difficulty arises from the fact that only in intermediate-coupling situations can the eikonal method describe accurately the large-angle scattering by the static potential itself.[18,43] Thus, it is preferable to treat the static potential exactly if one wants to account correctly for large-angle scattering.

In order to avoid the above-mentioned difficulties associated with the use of the eikonal approximation, we have therefore elected to solve Eq. (2.10) approximately by following another procedure. We first use the properties of the Born and Glauber series[1-3] to obtain a local approximation to the optical potential through second order, and then perform a partial wave analysis of the resulting Schrödinger equation. The main problem is thus the determination of this local optical potential through second order. It is to this question that we now turn our attention.

We begin by considering the first-order or static potential defined in Eq. (2.4). We use the Hartree-Fock wave function[44]

$$|0\rangle = (Z!)^{-1/2} A\,|\phi_{n_1}(1)\rangle\,|\phi_{n_2}(2)\rangle \cdots |\phi_{n_Z}(Z)\rangle\,, \qquad (2.11)$$

where A is the familiar antisymmetrizing operator and the subscripts n_i denote a set of quantum numbers, including spin. Using Eq. (2.11), one can evaluate the matrix element of Eq. (2.4) in a completely straightforward manner; one finds, of course, just a sum of contributions from each Hartree-Fock orbital. The static potentials obtained in this way are very simple in form. They behave like ZQ/r at small distances and fall off exponentially outside a distance of the order of the size of the atom. Because of the strong Coulomb potential at small distances, one expects that the static potential will play a very important role in large-angle scattering.

Now we turn to the evaluation of the second-order part of the potential. Equation (2.6) for $V^{(2)}$ is difficult to deal with because of its nonlocal character. However, it can be shown that a very reasonable local approximation to $V^{(2)}$ can be obtained. Let us write

$$V^{(2)} = V_{\rm pol} + iV_{\rm abs}\,, \qquad (2.12)$$

where $V_{\rm pol}$ and $V_{\rm abs}$ are purely real but energy dependent. In a previous paper [see Eq. (2.25) of II] we have obtained the following expression for $V_{\rm pol}$:

$$V_{\rm pol}(k,r) = -\frac{\pi}{2ka^3\rho}\langle 0|\,\mathfrak{z}^2\,|0\rangle \times \left(I_0(\rho) - L_0(\rho) - \frac{1}{\rho}[I_1(\rho) - L_1(\rho)]\right), \qquad (2.13)$$

where $\rho = r/a, a = k/2\Delta$, $\mathfrak{z}$ denotes the sum of all z coordinates of the bound electrons, I_n is a modified Bessel function, and L_n is a modified Struve function. The second-order potential $V_{\rm pol}$ dominates the optical potential at large distances, where it has the form

$$V_{\rm pol} = -\frac{\overline{\alpha}}{2r^4}\left(1 + \frac{6a^2}{r^2} + \frac{135a^4}{r^4} + \cdots\right), \qquad (2.14)$$

$\overline{\alpha}$ being the dipole polarizability of the target atom obtained in the closure approximation. That is,

$$\overline{\alpha} = 2\langle 0|\,\mathfrak{z}^2\,|0\rangle/\Delta\,. \qquad (2.15)$$

Thus, $V_{\rm pol}$ has precisely the polarization form which one would expect at large distances. The quantity $a = k/2\Delta$ acts as the cutoff radius for this potential. This long-range potential will have its maximum effect at small angles, where it is responsible for the rapid, linear rise of the differential cross section. It is worth noting that at large r our polarization potential $V_{\rm pol}$ falls below its asymptotic value $-\overline{\alpha}/2r^4$. This is just the opposite of what would be obtained from a phenomenological Buckingham potential of the form $-\overline{\alpha}/2(r^2+a^2)^2$, and is not surprising since Buckingham's cutoff procedure is by no means unique. A detailed discussion of the long-range behavior of an effective potential related (but not equivalent) to the optical potential has been given by Huo.[45]

In order to determine the absorption potential $V_{\rm abs}$ we shall proceed in an indirect manner. We begin by noting that if we treat $V_{\rm st} + V_{\rm pol} + iV_{\rm abs}$ by the eikonal method, then we obtain for the optical-eikonal (OE) amplitude [see Eq. (2.10) of II]

$$f_{\rm OE} = \frac{k}{2\pi i}\int d^2\vec{b}\, e^{i\vec{K}\cdot\vec{b}} \times \{\exp[i(V_0\chi_{\rm st} + V_0^2\chi_{\rm pol} + iV_0^2\chi_{\rm abs})] - 1\}\,, \qquad (2.16)$$

where

$$V_0\chi_{\rm st}(k,\vec{b}) = -\frac{1}{k}\int_{-\infty}^{+\infty} V_{\rm st}(\vec{b},z)\,dz\,, \qquad (2.17a)$$

$$V_0^2\chi_{\rm pol}(k,\vec{b}) = -\frac{1}{k}\int_{-\infty}^{+\infty} V_{\rm pol}(k,\vec{b},z)\,dz\,, \qquad (2.17b)$$

$$V_0^2\chi_{\rm abs}(k,\vec{b}) = -\frac{1}{k}\int_{-\infty}^{+\infty} V_{\rm abs}(k,\vec{b},z)\,dz\,. \qquad (2.17c)$$

Here we have written V_0 as the strength of the Coulomb potential. It is of course equal to 1 in atomic units but we will write it explicitly for a short time in order to make the derivation given below more transparent. Clearly, according to Eqs. (2.4) and (2.5) $V_{\rm st}$ contains one power of V_0 while $V^{(2)}$ contains two powers.

If, on the other hand, we solve the electron-(positron-) atom scattering problem by using the many-body Glauber approach,[46] we find that the Glauber amplitude is given by

$$f_G = \frac{k}{2\pi i}\int d^2\vec{b}\, e^{i\vec{K}\cdot\vec{b}}\langle 0|(e^{iV_0\chi_G} - 1)|0\rangle\,, \qquad (2.18)$$

where the Glauber phase-shift function χ_G is given by

$$\chi_G(k,\vec{b},\vec{b}_1,\ldots,\vec{b}_Z) = -\frac{Q}{k}\sum_{i=1}^{Z}\hat{\chi}_G(\vec{b}-\vec{b}_i) \qquad (2.19)$$

and we have introduced the k-independent quantities

$$\hat{\chi}_G(\vec{b}-\vec{b}_i) = \ln[(\vec{b}-\vec{b}_i)^2/b^2]\,, \qquad (2.20)$$

$\vec{b}_i$ being the coordinate of the ith atomic electron in the "impact-parameter" plane which contains $\vec{K}$ and is perpendicular to the collision plane. If we now expand Eq. (2.18) in powers of V_0 we have

$$f_G = \frac{k}{2\pi i}\int d^2\vec{b}\, e^{i\vec{K}\cdot\vec{b}} \times (iV_0\langle 0|\chi_G|0\rangle - \tfrac{1}{2}V_0^2\langle 0|\chi_G^2|0\rangle + \cdots). \tag{2.21}$$

Similarly, expanding Eq. (2.16) we find that

$$f_{OE} = \frac{k}{2\pi i}\int d^2\vec{b}\, e^{i\vec{K}\cdot\vec{b}}\,(iV_0\chi_{st} + iV_0^2\chi_{pol} - V_0^2\chi_{abs} - \tfrac{1}{2}V_0^2\chi_{st}^2 + \cdots). \tag{2.22}$$

If we ask that Eqs. (2.21) and (2.22) should be equivalent through second order, then upon equating the coefficients of V_0 and V_0^2 in these two equations we find that

$$\chi_{st} = \langle 0|\chi_G|0\rangle = -\frac{Q}{k}\langle 0|\sum_{i=1}^{Z}\hat{\chi}_G(\vec{b}-\vec{b}_i)|0\rangle\,, \tag{2.23a}$$

$$\begin{aligned}\chi_{abs}^G &= \tfrac{1}{2}[\langle 0|\chi_G^2|0\rangle - \chi_{st}^2] \\ &= \frac{1}{2k^2}\left[\langle 0|\sum_{i=1}^{Z}\sum_{j=1}^{Z}\hat{\chi}_G(\vec{b}-\vec{b}_i)\hat{\chi}_G(\vec{b}-\vec{b}_j)|0\rangle - 2\left(\langle 0|\sum_{i=1}^{Z}\hat{\chi}_G(\vec{b}-\vec{b}_i)|0\rangle\right)^2\right],\end{aligned} \tag{2.23b}$$

$$\chi_{pol} = 0\,, \tag{2.23c}$$

where the superscript G refers to the fact that χ_{abs}^G is only a (Glauber) approximation to χ_{abs}. No such superscript is necessary in the case of χ_{st}, since χ_{st} obtained in this manner is in fact exact. We note that Eq. (2.23c) merely expresses the fact, which has been commented on elsewhere,[1-3] that the Glauber method is seriously deficient inasmuch as it gives no real part to the scattering amplitude in second order.[1-3] However, the Glauber approximation has been shown[1] to do very well for the imaginary part of the amplitude, except at small angles. We shall therefore use Eq. (2.23b) to determine the quantity χ_{abs}^G, which can be used to obtain an absorption potential V_{abs}^G. The modifications required in order to deal properly with the small-angle region will be discussed at a later stage. Thus, returning to Eq. (2.23b) and using the Hartree-Fock wave function (2.11), we obtain after some straightforward algebra

$$\begin{aligned}\chi_{abs}^G = \frac{1}{2k^2}\Big(\sum_{i=1}^{Z}[\langle\phi_{n_i}(\vec{r}')|\hat{\chi}_G^2(\vec{b}-\vec{b}')|\phi_{n_i}(\vec{r}')\rangle - |\langle\phi_{n_i}(\vec{r}')|\hat{\chi}_G(\vec{b}-\vec{b}')|\phi_{n_i}(\vec{r}')\rangle|^2] \\ - 2\sum_{i\neq j}|\langle\phi_{n_i}(\vec{r}')|\hat{\chi}_G(\vec{b}-\vec{b}')|\phi_{n_j}(\vec{r}')\rangle|^2\Big).\end{aligned} \tag{2.24}$$

The last term is the exchange contribution to χ_{abs}^G due to the fact that we are using Hartree-Fock rather than Hartree wave functions. This should not be confused with exchange effects involving the incident electron and the target electrons which have not yet been included in our optical potential.

Let us illustrate Eq. (2.24) by two examples. For a helium target, we have

$$\chi_{abs}^{G,He} = (1/k^2)(\langle 1s|\hat{\chi}_G^2|1s\rangle - |\langle 1s|\hat{\chi}_G|1s\rangle|^2)\,, \tag{2.25}$$

where the spin algebra has been performed so that $|1s\rangle$ refers to a purely spacial orbital. For neon, exchange terms come in to give a slightly more tedious expression:

$$\begin{aligned}\chi_{abs}^{G,Ne} = (1/k^2)(&\langle 1s|\hat{\chi}_G^2|1s\rangle - |\langle 1s|\hat{\chi}_G|1s\rangle|^2 + \langle 2s|\hat{\chi}_G^2|2s\rangle - |\langle 2s|\hat{\chi}_G|2s\rangle|^2 \\ &+ 2\langle 2p_+|\hat{\chi}_G^2|2p_+\rangle - 2|\langle 2p_+|\hat{\chi}_G|2p_+\rangle|^2 + \langle 2p_0|\hat{\chi}_G^2|2p_0\rangle - |\langle 2p_0|\hat{\chi}_G|2p_0\rangle|^2 \\ &- 2|\langle 1s|\hat{\chi}_G|2s\rangle|^2 - 4|\langle 1s|\hat{\chi}_G|2p_+\rangle|^2 - 4|\langle 2s|\hat{\chi}_G|2p_+\rangle|^2 - 2|\langle 2p_+|\hat{\chi}_G|2p_-\rangle|^2).\end{aligned} \tag{2.26}$$

Here we have made use of the fact that

$$\langle n|\hat{\chi}_G|2p_0\rangle = 0 \tag{2.27}$$

when $n = 1, 2s, 2p_+, 2p_-$, since then the z integration in the inner product yields identically zero by symmetry. Also, it is obvious that

$$|\langle ns|\hat{\chi}_G|2p_+\rangle| = |\langle ns|\hat{\chi}_G|2p_-\rangle|\,, \tag{2.28}$$

so $2p_-$ matrix elements have been largely eliminated in Eq. (2.26). Notice in Eqs. (2.25) and (2.26) that terms in $\ln b$ at small b coming from $\langle n|\hat{\chi}_G^2|n\rangle$ are exactly canceled by similar terms from $|\langle n|\hat{\chi}_G|n\rangle|^2$, so that for small values of the impact parameter χ_{abs}^G tends to a constant. Thus, as we should expect on physical grounds, the dominant large-angle scattering will come from χ_{st}, which is proportional to $\ln b$ for small b, reflecting the r^{-1} singularity in V_{st}.

We now proceed to obtain an absorption potential from χ_{abs}^G. If we assume that there exists a local, spherically symmetric Glauber absorption potential $V_{abs}^G(k, r)$, then we may write from Eq. (2.17c) (with $V_0 = 1$)

$$\chi_{\rm abs}^G(k,b) = -\frac{1}{k}\int_{-\infty}^{+\infty} V_{\rm abs}^G(k,(b^2+z^2)^{1/2})\,dz$$
$$= -\frac{2}{k}\int_b^\infty (r^2-b^2)^{-1/2} V_{\rm abs}^G(k,r)\,r\,dr\,. \qquad (2.29)$$

This is an Abel integral equation which is readily solved for $V_{\rm abs}^G$, giving

$$V_{\rm abs}^G(k,r) = \frac{k}{\pi}\int_r^\infty (b^2-r^2)^{-1/2}\frac{d}{db}\chi_{\rm abs}^G(k,b)\,db\,. \qquad (2.30)$$

It is worth noting that $\chi_{\rm abs}^G$ is proportional to k^{-2} [see Eq. (2.24)], so that $V_{\rm abs}^G$ actually decreases as k^{-1} when k increases.

With $\chi_{\rm abs}^G$ determined from Eq. (2.24), one may then obtain $V_{\rm abs}^G(k,r)$ by elementary numerical methods. However, as remarked earlier, the Glauber amplitude suffers from serious defects at small angles, and these defects translate into an incorrect behavior of $V_{\rm abs}^G(k,r)$ for large r. This arises simply from the fact that $\chi_{\rm abs}^G$, as obtained above, falls off like b^{-2} for large b, as may easily be seen from Eqs. (2.20) and (2.24). However, it is known from the work of Joachain and Mittleman[14] that for large b the true $\chi_{\rm abs}(k,b)$ falls off exponentially, the precise large-b behavior of $\chi_{\rm abs}(k,b)$ being given by[47] $(\delta/b)e^{-\delta b}$, where $\delta=a^{-1}=2\Delta/k$. Therefore the spurious b^{-2} behavior of $\chi_{\rm abs}^G$, as obtained from Eq. (2.24), gives rise to an absorption potential $V_{\rm abs}^G(k,r)$ which falls off like r^{-3} for large r instead of the much faster rate $(\delta/r)^{3/2}e^{-\delta r}$ corresponding to the $\chi_{\rm abs}$ of Ref. 14.

In order to eliminate this spurious behavior, the following procedure was adopted: In I we discussed the contribution to the second Born term $\bar f_{B2}$, (in the closure approximation) from an orbital $(Z^{*3}/\pi)^{1/2}e^{-Z^*r}$. It was also shown in I that if one looks at the leading part of $\mathrm{Im}\bar f_{B2}$ in powers of k^{-1} the following simple expression is obtained:

$$\mathrm{Im}\bar f_{B2} = \frac{4}{k}\left(\ln\frac{K^2+4Z^{*2}}{\delta Z^*} - \frac{K}{(K^2+\delta^2)^{1/2}}\ln\frac{K+(K^2+\delta^2)^{1/2}}{\delta}\right)$$
$$\times\frac{K^2+8Z^{*2}}{(K^2+4Z^{*2})^2} + \frac{2}{k}\frac{K^2-4Z^{*2}}{(K^2+4Z^{*2})^2}\,. \qquad (2.31)$$

Furthermore, it is easy to show[48] that the Glauber approximation to this second-order term, $\mathrm{Im}\bar f_{G2}$, is given by Eq. (2.31) but with $\delta=0$, i.e.,

$$\mathrm{Im}\bar f_{G2} = \frac{4}{k}\frac{K^2+8Z^{*2}}{(K^2+4Z^{*2})^2}\ln\frac{K^2+4Z^{*2}}{2KZ^*} + \frac{2}{k}\frac{K^2-4Z^{*2}}{(K^2+4Z^{*2})^2}\,. \qquad (2.32)$$

Thus, if one transforms this back into position space in an obvious way one obtains precisely that part of $V_{\rm abs}^G(k,r)$ coming from the orbital in question. If we now form the difference $f_{\rm corr} = \mathrm{Im}\bar f_{B2} - \mathrm{Im}\bar f_{G2}$ we find that

$$f_{\rm corr}(K) = \frac{4}{k}\left(\ln K + \ln\frac{2}{\delta}\frac{K}{(K^2+\delta^2)^{1/2}}\ln\frac{K+(K^2+\delta^2)^{1/2}}{\delta}\right)$$
$$\times\frac{K^2+8Z^{*2}}{(K^2+4Z^{*2})^2}\,. \qquad (2.33)$$

The only Z^* dependence is contained in the simple expression multiplying the large parentheses in Eq. (2.33), and thus it is a straightforward matter to obtain $f_{\rm corr}$ for a more-complicated orbital by simply differentiating with respect to Z^*. Adding up the contribution from each orbital, one then gets a quantity $f_{\rm corr}^{\rm tot}(K)$ which should be used to correct the imaginary part of the Glauber amplitude. (Note that by summing over the closed p shell, we may neglect the angular dependence of the p orbitals.) According to our previous discussion, if we define $V_{\rm corr}$ via

$$-\frac{1}{2\pi}\int V_{\rm corr}(k,r)e^{i\vec K\cdot\vec r}\,d\vec r = f_{\rm corr}^{\rm tot}(K)\,, \qquad (2.34)$$

then

$$V_{\rm corr}(k,r) = -\frac{1}{\pi r}\int_0^\infty K\sin Kr\, f_{\rm corr}^{\rm tot}(K)\,dK \qquad (2.35)$$

is precisely the quantity which should be added to $V_{\rm abs}^G(k,r)$ in order to correct the large-r behavior. Hence, the true absorption potential $V_{\rm abs}(k,r)$ will be given by

$$V_{\rm abs}(k,r) = V_{\rm abs}^G(k,r) + V_{\rm corr}(k,r)\,. \qquad (2.36)$$

There is a small modification to this procedure owing to the fact that, as can be seen from Eq. (2.29) of I, there are terms contributing to $\mathrm{Im}\bar f_{B2}$ which arise from interference between different orbitals. Such contributions are mostly of the potential scattering type and cause no difficulty near the forward direction. Only the small interference between s and p orbitals needs some attention; a procedure nearly identical to the one given above yields a small modification of $f_{\rm corr}^{\rm tot}$ and hence of $V_{\rm corr}$. Details are given in the Appendix.

We may remark in passing that it is the presence of these extra terms coming from interference between orbitals which makes it convenient to use the Glauber approximation for the imaginary part of the second-order term rather than directly Fourier transforming $\mathrm{Im}\bar f_{B2}$.

In order to obtain a general picture of the behavior of $V_{\rm abs}$ as a function of r let us look back at Eq. (2.33) for $f_{\rm corr}$. The three terms in the large parentheses have very distinct behaviors when transformed into position space. The first term ($\ln K$) gives rise to a function which for large r takes the form of a power series in r^{-1}, beginning with r^{-3}. This is to be expected since an inspection of Eq. (2.32) shows that this is the only term in the Glauber amplitude which will give rise to anything other than terms which fall off like $e^{-Z^* r}$ in position space.[49] Therefore, in subtracting this term from the Glauber amplitude one eliminates all terms containing inverse powers of r.

The second term $[\ln(2/\delta) = \ln(k/\Delta)]$ is just a constant and thus gives rise to a term, proportional to $k^{-1}\ln k$, which also falls off in position space like $e^{-Z^* r}$. The third term in the large parentheses varies on a scale set by δ. Thus, it is expected to fall off in position space like $e^{-\delta r}$. That this is indeed the case may be seen as follows. Using Eq. (2.35) we see that the term in question will give a contribution to V_{corr} which is given by

$$V_{\text{corr}}^{(3)} = \frac{4}{\pi k r}\int_0^\infty K \sin Kr \frac{K}{(K^2+\delta^2)^{1/2}} \times \ln\left(\frac{K+(K^2+\delta^2)^{1/2}}{\delta}\right)\frac{K^2+8Z^{*2}}{(K^2+4Z^{*2})^2}\,dK. \tag{2.37}$$

Making the change of variable $K = \delta \sinh y$, we get

$$V_{\text{corr}}^{(3)} = -\frac{4}{\pi k r}\frac{d^2}{dr^2}\int_0^\infty \sin(\delta r \sinh y)\, y \times \frac{(8Z^{*2}+\delta^2\sinh^2 y)}{(4Z^{*2}+\delta^2\sinh^2 y)^2}\,dy. \tag{2.38}$$

Clearly, if δr is large, we may neglect the terms in δ^2 in the final ratio in the integrand of Eq. (2.38). Hence,

$$V_{\text{corr}}^{(3)} \simeq \frac{2}{\pi Z^{*2} k r}\frac{d^2}{dr^2}\int_0^\infty \sin(\delta r \sinh y)\, y\, dy. \tag{2.39}$$

This integral is elementary, giving

$$V_{\text{corr}}^{(3)} \simeq -\frac{\delta^2}{Z^{*2} k r}\left(K_0(\delta r) + \frac{K_1(\delta r)}{\delta r}\right), \tag{2.40}$$

where K_0 and K_1 are modified Bessel functions. Since δr is large, we may write this as

$$V_{\text{corr}}^{(3)} \simeq \left(\frac{\pi}{2}\right)^{1/2}\frac{1}{Z^{*2} k}\left(\frac{\delta}{r}\right)^{3/2} e^{-\delta r}, \tag{2.41}$$

in agreement with the result of Joachain and Mittleman.[14] Thus we see that the small-K behavior of $\text{Im}\bar{f}_{B2}$ is governed by a potential having two very different terms, one falling off exponentially with a scale set by the size of the atom, the other falling off exponentially with a scale set by δ^{-1}, which is large in the intermediate- and high-energy regime. Any phenomenological attempt to represent absorption by either a simple long-range potential or a simple short-range potential will thus suffer from serious difficulties.

We now turn to the problem of exchange effects between the incident and atomic electrons. Several attempts have been made in the past to construct a local pseudopotential to mimic the effects of exchange in the optical model. We may mention the pioneering work of Mittleman and Watson[5] and the recent work of Furness and McCarthy.[16] Both of these pseudopotentials have the virtue of yielding an exchange amplitude which agrees with the Ochkur amplitude at high energy. Higher-order effects are somewhat different in the two models, but since these are poorly understood at the present time we have elected to use the pseudopotential of Mittleman and Watson, which is somewhat simpler to use than that of Furness and McCarthy. Moreover, in the energy range under consideration here, these two methods give very similar results, particularly at the higher energies. This pseudopotential may be written as

$$V_{\text{opt}}^{\text{ex}} = -\left(k p_f - \frac{(k^2 - p_F^2)}{2}\ln\left|\frac{k+p_F}{k-p_F}\right|\right)\frac{1}{\pi k}, \tag{2.42a}$$

where p_F is the Fermi momentum and is given by

$$p_F = [3\pi^2\rho(r)]^{1/3}. \tag{2.42b}$$

Here $\rho(r)$ is the (spherically symmetric) charge distribution of the target atom, i.e., the integral over all space of $\rho(r)$ is equal to Z. Consistent with our determination of the direct parts of the optical potential, we have evaluated $\rho(r)$ in the Hartree-Fock approximation, using Eq. (2.11) for the ground-state wave function. The potential of Eq. (2.42) is obviously highly localized, falling off rapidly outside a typical atomic distance. In fact, if $p_F/k \ll 1$ we have for V_{ex} the simple expression

$$V_{\text{opt}}^{\text{ex}} \simeq -2\pi\rho(r)/k^2, \tag{2.43}$$

which explicitly shows the rapid falloff of $V_{\text{opt}}^{\text{ex}}$. If one treats $V_{\text{opt}}^{\text{ex}}$ in first Born approximation one obtains the familar Ochkur result.[1]

Finally, combining the above results we write our local approximation to the optical potential as

$$\mathcal{V}_{\text{opt}} = V_{\text{opt}}^{d} + V_{\text{opt}}^{\text{ex}} = V_{\text{st}} + V_{\text{pol}} + iV_{\text{abs}} + V_{\text{opt}}^{\text{ex}}, \tag{2.44}$$

where V_{st}, V_{pol}, V_{abs}, and $V_{\text{opt}}^{\text{ex}}$ are given, respectively, by Eqs. (2.4), (2.13), (2.36), and (2.42).

It is perhaps worthwhile to close this section by commenting in some detail on the connection between the optical potential given in Eq. (2.44) and the EBS method of I; this connection is straightforward and illuminates some of the approximations made in this paper. First, the term V_{st} of the optical potential, treated in first Born approximation, gives exactly the term $\bar{f}_{B1}$ of the EBS method. Second, V_{abs}, treated in first Born approximation and combined with the imaginary contribution of V_{st} acting twice in perturbation theory, gives the leading piece of $\mathrm{Im}\bar{f}_{B2}$ (in powers of k^{-1}). Similarly, V_{pol}, treated in first Born approximation and combined with the real contribution of V_{st} acting twice in perturbation theory, gives a good approximation to $\mathrm{Re}\bar{f}_{B2}$. It is not completely correct to leading order in k^{-1}, but it does give the leading small-angle and large-angle behaviors correctly; in II it was shown that this approximation to $\mathrm{Re}\bar{f}_{B2}$ in helium was good to about 15% at intermediate angles and much better than that at small and large angles. Third, the real part of the term coming from V_{st} acting three times in perturbation theory, when combined with the term representing the interference between V_{st} and V_{abs} in second order, gives an approximation to $\mathrm{Re}\bar{f}_{B3}$ which was also studied in II. At angles greater than 30°, this approximation is good to better than 10%, but at small angles it deteriorates rapidly, since long-range, third-order potentials are completely missing from our treatment. Fortunately, this error in $\bar{f}_{B3}$ comes primarily in the region where the second-order terms are very large. Finally, V_{opt}^{ex} treated in first Born approximation duplicates in the large-k limit the Ochkur approximation to the first Born exchange amplitude used in I.

Thus, the optical potential contains all the ingredients of the EBS method, the worst errors occurring because of the omission of the third-order term in $\mathcal{V}_{opt}$. Of course in treating the optical potential of Eq. (2.44) exactly by the method of partial waves, one generates approximations to all terms of perturbation theory, not just those used in the EBS method. This feature is a very important advantage when one applies the optical-potential method to complex atoms.

III. ELECTRON AND POSITRON SCATTERING BY HELIUM

Using the Hartree-Fock orbital given in Ref. 44, we have evaluated the optical potential for electron scattering by helium. The corresponding optical potential for positron-helium scattering is obtained simply by changing the sign of V_{st} and omitting V_{opt}^{ex}. Our results for electron-helium scattering at energies ranging from 100 to 700 eV are given in Table I. Detailed comparisons with the recent experimental results of Bromberg,[23,26] Crooks and Rudd,[24] Oda *et al.*,[25] Sethuraman *et al.*,[27] and Jansen *et al.*[28] are given in Tables II and III. The agreement between the last three sets of experimental values shown in Table II suggests that the results of Crooks and Rudd at 200 eV might be slightly on the high side, especially at small angles. The agreement between our optical-model results and the experimental results of Refs. 26–28 at 200 eV and Refs. 23, 25, 26, and 28 at 500 eV is seen to be excellent.

Also, there is good agreement between the previously obtained EBS results of I and the present optical-model results, the agreement

TABLE I. Differential cross sections (in a_0^2/sr) for the elastic scattering of electrons by helium in the energy range 100–700 eV, as obtained from the present *ab initio* optical-model theory. The numbers in parentheses indicate powers of 10.

θ (deg)	Energy (eV) 100	200	300	400	500	700
0	4.03	2.99	2.48	2.18	1.98	1.72
5	3.22	1.98	1.40	1.11	9.34 (−1)	7.49 (−1)
10	2.43	1.25	8.45 (−1)	6.64 (−1)	5.63 (−1)	4.50 (−1)
15	1.78	8.33 (−1)	5.55 (−1)	4.30 (−1)	3.56 (−1)	2.66 (−1)
20	1.29	5.75 (−1)	3.75 (−1)	2.80 (−1)	2.23 (−1)	1.54 (−1)
25	9.51 (−1)	4.06 (−1)	2.55 (−1)	1.83 (−1)	1.40 (−1)	9.03 (−2)
30	7.06 (−1)	2.91 (−1)	1.75 (−1)	1.21 (−1)	8.91 (−2)	5.45 (−2)
35	5.30 (−1)	2.11 (−1)	1.22 (−1)	8.12 (−2)	5.83 (−2)	3.43 (−2)
40	4.04 (−1)	1.55 (−1)	8.65 (−2)	5.60 (−2)	3.93 (−2)	2.24 (−2)
50	2.44 (−1)	8.86 (−2)	4.64 (−2)	2.87 (−2)	1.95 (−2)	1.07 (−2)
60	1.57 (−1)	5.43 (−2)	2.71 (−2)	1.63 (−2)	1.08 (−2)	5.76 (−3)
70	1.08 (−1)	3.57 (−2)	1.71 (−2)	1.00 (−2)	6.58 (−3)	3.44 (−3)
80	7.89 (−2)	2.49 (−2)	1.15 (−2)	6.65 (−3)	4.31 (−3)	2.22 (−3)
90	6.11 (−2)	1.84 (−2)	8.24 (−3)	4.68 (−3)	3.01 (−3)	1.54 (−3)
100	4.98 (−2)	1.42 (−2)	6.19 (−3)	3.47 (−3)	2.22 (−3)	1.13 (−3)
120	3.74 (−2)	9.51 (−3)	3.97 (−3)	2.19 (−3)	1.38 (−3)	6.96 (−4)
140	3.17 (−2)	7.28 (−3)	2.94 (−3)	1.60 (−3)	1.01 (−3)	5.04 (−4)
160	2.91 (−2)	6.24 (−3)	2.47 (−3)	1.34 (−3)	8.38 (−4)	4.19 (−4)
180	2.83 (−2)	5.94 (−3)	2.33 (−3)	1.26 (−3)	7.90 (−4)	3.94 (−4)

TABLE II. Comparison of various theoretical and experimental differential cross sections for elastic electron-helium scattering at an incident-electron energy of 200 eV. All results are in a_0^2/sr. Numbers in parentheses are powers of ten.

			Experimental values		
(deg)	Present theory	Crooks and Rudd (Ref. 24)	Bromberg (Ref. 26)	Sethuraman *et al.* (Ref. 27)	Jansen *et al.* (Ref. 28)
0	2.99	···	···	···	···
5	1.98	···	1.73	···	1.68
10	1.25	1.93	1.12	···	1.08
15	8.33 (−1)	···	···	···	7.39 (−1)
20	5.75 (−1)	7.13 (−1)	5.27 (−1)	···	5.28 (−1)
25	4.06 (−1)	···	3.78 (−1)	···	3.85 (−1)
30	2.91 (−1)	3.25 (−1)	2.76 (−1)	2.63 (−1)	2.81 (−1)
40	1.55 (−1)	···	1.52 (−1)	1.57 (−1)	1.51 (−1)
50	8.86 (−2)	1.03 (−1)	8.91 (−2)	9.30 (−2)	8.85 (−2)
60	5.43 (−2)	···	5.57 (−2)	5.38 (−2)	···
70	3.57 (−2)	4.23 (−2)	3.72 (−2)	3.57 (−2)	···
80	2.49 (−2)	···	2.63 (−2)	2.47 (−2)	···
90	1.84 (−2)	2.33 (−2)	1.90 (−2)	1.77 (−2)	···
100	1.42 (−2)	···	1.45 (−2)	1.40 (−2)	···
110	1.14 (−2)	1.41 (−2)	1.18 (−2)	1.15 (−2)	···
120	9.51 (−3)	···	···	9.8 (−3)	···
130	8.20 (−3)	1.05 (−2)	···	8.0 (−3)	···
140	7.28 (−3)	···	···	6.8 (−3)	···
150	6.65 (−3)	8.43 (−3)	···	6.0 (−3)	···
160	6.24 (−3)	···	···	···	···
170	6.01 (−3)	···	···	···	···
180	5.94 (−3)	···	···	···	···

TABLE III. Comparison of various theoretical and experimental differential cross sections for elastic electron-helium scattering at an incident-electron energy of 500 eV. All results are in a_0^2/sr. The values in brackets have been interpolated from experimental results at nearby angles. Numbers in parentheses are powers of 10.

				Experimental values		
θ (deg)	Present theory	Bromberg (Ref. 23)	Bromberg (Ref. 26)	Oda *et al.* (Ref. 25)	Sethuraman *et al.* (Ref. 27)	Jansen *et al.* (Ref. 28)
0	1.98	···	···	···	···	···
5	9.34 (−1)	9.62 (−1)	9.47 (−1)	···	···	9.06 (−1)
10	5.63 (−1)	5.76 (−1)	5.71 (−1)	5.87 (−1)	···	5.50 (−1)
15	3.56 (−1)	···	[3.63 (−1)]	3.79 (−1)	···	3.55 (−1)
20	2.23 (−1)	2.28 (−1)	2.26 (−1)	2.28 (−1)	···	2.29 (−1)
25	1.40 (−1)	1.42 (−1)	1.43 (−1)	1.41 (−1)	···	1.46 (−1)
30	8.90 (−2)	9.22 (−2)	9.15 (−2)	9.22 (−2)	9.41 (−2)	9.33 (−2)
40	3.39 (−2)	4.09 (−2)	4.10 (−2)	4.28 (−2)	4.13 (−2)	4.12 (−2)
50	1.95 (−2)	2.05 (−2)	2.02 (−2)	2.05 (−2)	1.85 (−2)	2.03 (−2)
60	1.08 (−2)	1.11 (−2)	1.13 (−2)	1.16 (−2)	1.11 (−2)	···
70	6.58 (−3)	···	6.87 (−3)	[7.20 (−3)]	6.10 (−3)	···
80	4.30 (−3)	···	4.48 (−3)	[4.75 (−3)]	3.83 (−3)	···
90	3.01 (−3)	···	3.13 (−3)	[3.15 (−3)]	2.54 (−3)	···
100	2.22 (−3)	···	2.30 (−3)	[2.10 (−3)]	1.78 (−3)	···
110	1.71 (−3)	···	1.79 (−3)	[1.51 (−3)]	1.31 (−4)	···
120	1.38 (−3)	···	···	[1.15 (−3)]	9.3 (−4)	···
130	1.16 (−3)	···	···	[9.50 (−4)]	7.6 (−4)	···
140	1.01 (−3)	···	···	[9.10 (−4)]	7.3 (−4)	···
150	9.04 (−4)	···	···	···	6.7 (−4)	···
160	8.38 (−4)	···	···	···	···	···
170	8.01 (−4)	···	···	···	···	···
180	7.90 (−4)	···	···	···	···	···

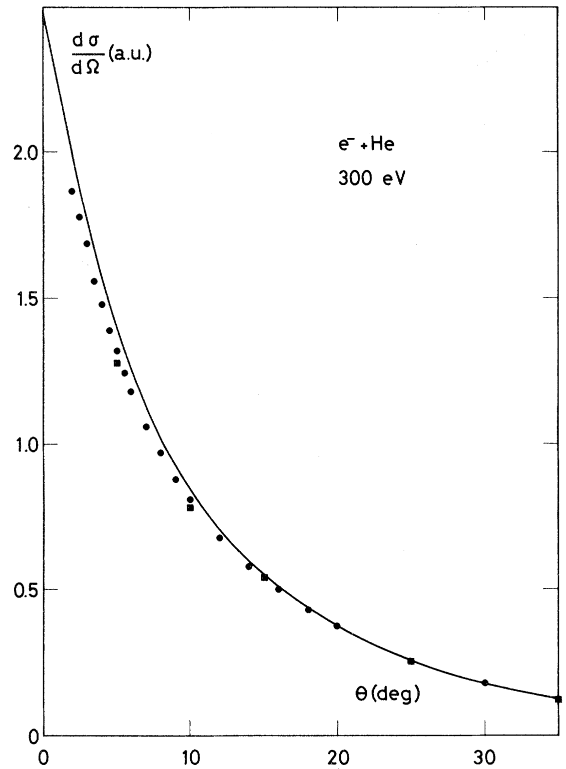

FIG. 1. Small-angle differential cross section for the elastic scattering of 300-eV electrons by helium. The solid curve is the optical-model result using Eq. (2.44) of this paper. The filled circles represent the experimental values of Ref. 26. The filled squares are the experimental results of Ref. 28.

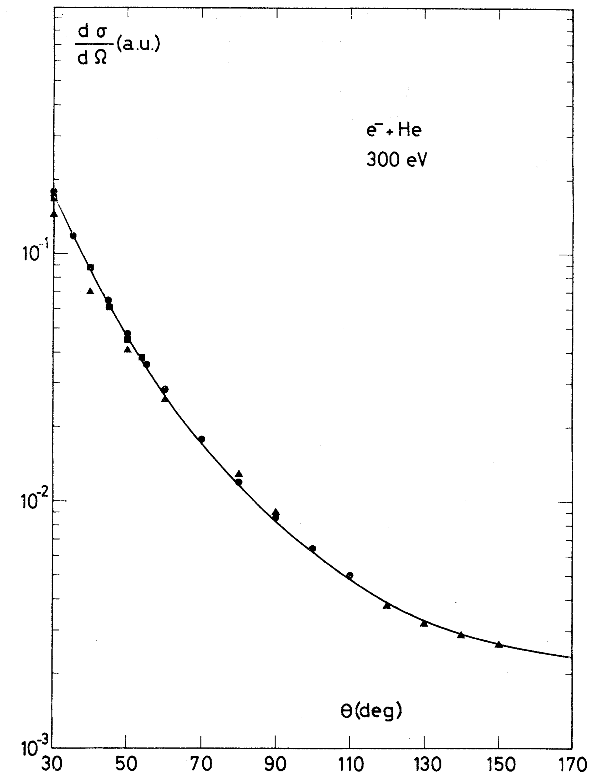

FIG. 2. Same as Fig. 1 but for large-angle scattering. The triangles are the experimental results of Ref. 27.

TABLE IV. Comparison of various differential cross sections (in a_0^2/sr) for electron-helium scattering at 400 eV, as obtained from several approximations. Numbers in parentheses are powers of 10.

(deg)	First Born approx.	Opt. model with V_{st} only	Opt. model with $V_{opt}^{d} = V_{st} + V_{pol}$, no exchange	Opt. model with $V_{opt}^{d} = V_{st} + V_{pol} + iV_{abs}$, no exchange	Opt. model with $V_{opt}^{d} = V_{st} + V_{pol} + iV_{abs}$, Ochkur exchange	Opt. model with $V_{opt} = V_{st} + V_{pol} + i\,V_{abs} + V_{opt}^{ex}$
0	6.28 (−1)	6.27 (−1)	1.54	2.00	2.17	2.18
5	5.83 (−1)	5.82 (−1)	7.71 (−1)	9.83 (−1)	1.09	1.11
10	4.75 (−1)	4.75 (−1)	5.31 (−1)	5.78 (−1)	6.58 (−1)	6.64 (−1)
15	3.51 (−1)	3.53 (−1)	3.76 (−1)	3.73 (−1)	4.28 (−1)	4.30 (−1)
20	2.45 (−1)	2.47 (−1)	2.58 (−1)	2.43 (−1)	2.79 (−1)	2.80 (−1)
25	1.66 (−1)	1.69 (−1)	1.75 (−1)	1.60 (−1)	1.82 (−1)	1.83 (−1)
30	1.12 (−1)	1.15 (−1)	1.19 (−1)	1.06 (−1)	1.20 (−1)	1.21 (−1)
40	5.34 (−2)	5.59 (−2)	5.73 (−2)	4.98 (−2)	5.52 (−2)	5.60 (−2)
50	2.76 (−2)	2.97 (−2)	3.03 (−2)	2.59 (−2)	2.82 (−2)	2.87 (−2)
60	1.57 (−2)	1.72 (−2)	1.76 (−2)	1.49 (−2)	1.59 (−2)	1.63 (−2)
70	9.51 (−3)	1.08 (−2)	1.10 (−2)	9.26 (−3)	9.76 (−3)	1.00 (−2)
80	6.24 (−3)	7.26 (−3)	7.41 (−3)	6.20 (−3)	6.35 (−3)	6.65 (−3)
90	4.36 (−3)	5.17 (−3)	5.28 (−3)	4.40 (−3)	4.54 (−3)	4.68 (−3)
100	3.21 (−3)	3.87 (−3)	3.96 (−3)	3.29 (−3)	3.37 (−3)	3.47 (−3)
120	2.00 (−3)	2.47 (−3)	2.53 (−3)	2.10 (−3)	2.13 (−3)	2.19 (−3)
140	1.45 (−3)	1.83 (−3)	1.87 (−3)	1.55 (−3)	1.57 (−3)	1.60 (−3)
160	1.21 (−3)	1.53 (−3)	1.57 (−3)	1.30 (−3)	1.31 (−3)	1.34 (−3)
180	1.14 (−3)	1.45 (−3)	1.48 (−3)	1.22 (−3)	1.24 (−3)	1.26 (−3)

TABLE V. Total cross sections (in units of a_0^2) for electron-helium scattering.

Energy (eV)	Theoretical values: Total Bethe–Born (Ref. 51)	EBS theory (Ref. 1)	Present theory	Experimental values: Brode (Ref. 29)	Normand (Ref. 30)	Jansen *et al.* (Ref. 28)	de Heer and Jansen (Ref. 31)
100	5.00	4.57	6.16	3.94	3.43	5.3	4.05
200	2.98	2.90	3.37	2.63	2.14	···	2.68
300	2.20	2.14	2.38	1.90	1.37	2.3	2.03
400	1.73	1.72	1.86	···	0.93	···	1.66
500	1.45	1.45	1.54	···	···	1.5	1.39
700	1.10	1.10	1.16	···	···	···	1.06

being poorest at large angles, where the convergence of perturbation theory is slowest. Since the optical model treats the static potential, which is very important in large-angle scattering, exactly to all orders of perturbation theory the optical model is more accurate than the eikonal-Born series method at large angles.

A graphical example of the agreement between experiment and theory is given in Figs. 1 and 2, which illustrate the situation at 300 eV. Figure 1 shows the small-angle region, and Fig. 2 shows the large-angle region. Once again, the agreement between the optical-model results and the experimental values obtained by various workers is excellent.

It is interesting to see how the various parts of the optical potential contribute to the differential cross section for elastic scattering by helium. Table IV gives the relevant information. We see that at large angles V_{pol} and V_{opt}^{ex} have very little effect, as we should expect from the work of Ref. 18. At small angles V_{pol} is particularly important, as was pointed out in Sec. II. The absorption potential plays a role at all angles; the fact that V_{abs} has a rather long range means that it has a significant effect in the small-angle region, while the fact that V_{abs} interferes with V_{st} in second order to give a real term of order k^{-2} means that it will also have a significant effect at large angles. Finally, it is clear from Table IV that it makes very little difference whether exchange effects are included via a pseudopotential or by directly adding the Ochkur amplitude as was done in the EBS treatment.[1]

Table V shows the total cross section σ_T, which is related to the imaginary part of the forward

TABLE VI. Differential cross sections (in a_0^2/sr) for the elastic scattering of positrons by helium in the energy range 100–500 eV, as obtained from the present *ab initio* optical-model theory. Numbers in parentheses are powers of 10.

θ (deg)	Energy (eV): 100	200	300	400	500
0	8.12 (−1)	6.69 (−1)	6.10 (−1)	5.79 (−1)	5.60 (−1)
2	7.52 (−1)	6.54 (−1)	6.29 (−1)	6.21 (−1)	6.19 (−1)
5	6.56 (−1)	5.87 (−1)	5.70 (−1)	5.59 (−1)	5.49 (−1)
10	5.00 (−1)	4.48 (−1)	4.25 (−1)	4.05 (−1)	3.86 (−1)
15	3.71 (−1)	3.31 (−1)	3.05 (−1)	2.78 (−1)	2.53 (−1)
20	2.77 (−1)	2.44 (−1)	2.13 (−1)	1.84 (−1)	1.59 (−1)
25	2.09 (−1)	1.78 (−1)	1.46 (−1)	1.20 (−1)	9.91 (−2)
30	1.59 (−1)	1.29 (−1)	1.00 (−1)	7.84 (−2)	6.24 (−2)
35	1.23 (−1)	9.37 (−2)	6.91 (−2)	5.21 (−2)	4.04 (−2)
40	9.51 (−2)	6.84 (−2)	4.84 (−2)	3.55 (−2)	2.69 (−2)
50	5.81 (−2)	3.78 (−2)	2.52 (−2)	1.78 (−2)	1.31 (−2)
60	3.65 (−2)	2.22 (−2)	1.43 (−2)	9.88 (−3)	7.19 (−3)
70	2.39 (−2)	1.40 (−2)	8.83 (−3)	6.01 (−3)	4.33 (−3)
80	1.64 (−2)	9.41 (−3)	5.85 (−3)	3.94 (−3)	2.82 (−3)
90	1.18 (−2)	6.69 (−3)	4.12 (−3)	2.75 (−3)	1.96 (−3)
120	5.77 (−3)	3.19 (−3)	1.92 (−3)	1.27 (−3)	8.99 (−4)
150	3.90 (−3)	2.13 (−3)	1.27 (−3)	8.36 (−4)	5.88 (−4)
180	3.44 (−3)	1.87 (−3)	1.11 (−3)	7.30 (−4)	5.12 (−4)

TABLE VII. Total cross sections (in units of a_0^2) for positron-helium scattering.

Energy (eV)	Theoretical values Total Bethe-Born (Ref. 51)	EBS theory (Ref. 1)	Present theory	Experimental values Coleman *et al.* (Ref. 33)	Jaduszliwer *et al.* (Ref. 34)	Dutton *et al.* (Ref. 35)
100	5.00	4.57	3.96	3.14	3.49	3.20
200	2.98	2.90	2.68	2.12	2.48	2.23
300	2.20	2.14	2.05	1.65	1.93	1.88
400	1.73	1.72	1.67	1.41	...	1.67
500	1.45	1.45	1.42	...	...	...

elastic amplitude via the equation

$$\sigma_T = (4\pi/k)\,\mathrm{Im} f_{\mathrm{el}}(\theta = 0). \tag{3.1}$$

Of the theoretical values shown, the Bethe-Born result[50] is closely related to the EBS result since in Ref. I the average excitation energy was chosen so that the imaginary part of the second Born term in the forward direction agreed with the corresponding Bethe-Born value of the *total* cross section[51] at 500 eV. This required an average excitation energy of 1.3 a.u. In this work we used an average excitation energy of 1.15 a.u., which gives the physically observed polarizability when used in Eq. (2.15). The agreement between the optical-model results and the EBS results is seen to be good at energies above 100 eV, the two differing typically by about 10%. The experimental values all agree fairly well with each other at the lower energies, but the values of Normand[30] seem to fall seriously on the low side at the higher energies. The last column of experimental results was obtained by de Heer and Jansen[31] by adding the large elastic and ionization cross sections, which are rather reliably known, to the excitation cross section, which are probably not as reliable but which are small in magnitude. These results of de Heer and Jansen are thus likely to be quite accurate. Agreement between the last column of Table V and our optical-model results is good down to about 200 eV but is clearly worsening rapidly as one goes to lower energies. This is perhaps not surprising since the optical model is essentially a perturbative technique when used in the *ab initio* spirit presented here; in addition, the omission of the third-order optical potential is likely to be particularly important at small angles. It would be interesting to add the real part of the third-order potential, which could be

TABLE VIII. Differential cross sections (in a_0^2/sr) for the elastic scattering of electrons by neon in the energy range 100–700 eV, as obtained from the present *ab initio* optical-model theory. Numbers in parentheses are powers of 10.

θ (deg)	Energy (eV) 100	200	300	400	500	700
0	14.7	15.2	15.0	14.8	14.6	14.3
5	12.1	11.0	9.73	8.80	8.15	7.36
10	9.22	7.09	5.75	5.04	4.62	4.12
15	6.57	4.37	3.41	2.93	2.64	2.25
20	4.45	2.67	2.01	1.69	1.49	1.21
25	2.89	1.61	1.18	9.76 (−1)	8.42 (−1)	6.64 (−1)
30	1.82	9.70 (−1)	7.03 (−1)	5.76 (−1)	4.96 (−1)	3.89 (−1)
35	1.12	5.89 (−1)	4.30 (−1)	3.58 (−1)	3.11 (−1)	2.48 (−1)
40	6.79 (−1)	3.66 (−1)	2.77 (−1)	2.38 (−1)	2.11 (−1)	1.71 (−1)
50	2.54 (−1)	1.64 (−1)	1.42 (−1)	1.31 (−1)	1.19 (−1)	9.69 (−2)
60	1.22 (−1)	9.55 (−2)	9.34 (−2)	8.84 (−2)	8.05 (−2)	6.32 (−2)
70	8.63 (−2)	6.93 (−2)	7.11 (−2)	6.68 (−2)	5.95 (−2)	4.46 (−2)
80	6.95 (−2)	5.71 (−2)	5.92 (−2)	5.43 (−2)	4.69 (−2)	3.35 (−2)
90	4.92 (−2)	5.22 (−2)	5.36 (−2)	4.72 (−2)	3.93 (−2)	2.67 (−2)
100	2.91 (−2)	5.39 (−2)	5.27 (−2)	4.37 (−2)	3.49 (−2)	2.24 (−2)
120	4.65 (−2)	7.94 (−2)	6.07 (−2)	4.33 (−2)	3.14 (−2)	1.80 (−2)
140	1.95 (−1)	1.28 (−1)	7.49 (−2)	4.65 (−2)	3.10 (−2)	1.62 (−2)
160	4.04 (−1)	1.77 (−1)	8.73 (−2)	4.96 (−2)	3.15 (−2)	1.56 (−2)
180	5.03 (−1)	1.97 (−1)	9.22 (−2)	5.09 (−2)	3.17 (−2)	1.54 (−2)

TABLE IX. Comparison of various theoretical and experimental differential cross sections for elastic electron-neon scattering at an incident-electron energy of 300 eV. All results are in a_0^2/sr. Numbers in parentheses are powers of 10.

	Theoretical values		Experimental values		
θ (deg)	First Born approx.	Present theory	Bromberg (Ref. 26)	Jansen *et al.* (Ref. 28)	Gupta and Rees (Ref. 40)
0	9.77	15.0	...	...	...
5	9.31	9.73	8.95	8.63	...
10	8.11	5.75	5.47	5.48	5.65
15	6.57	3.41	3.46	3.46	3.40
20	5.06	2.01	2.12	2.19	2.08
25	3.78	1.18	1.32	1.39	1.26
30	2.78	7.03 (−1)	8.39 (−1)	8.77 (−1)	8.65 (−1)
35	2.04	4.30 (−1)	5.51 (−1)	5.68 (−1)	5.59 (−1)
40	1.50	2.77 (−1)	3.68 (−1)	3.83 (−1)	3.86 (−1)
45	1.11	1.92 (−1)	2.64 (−1)	2.72 (−1)	3.04 (−1)
50	8.34 (−1)	1.42 (−1)	1.96 (−1)	2.03 (−1)	2.29 (−1)
55	6.36 (−1)	1.12 (−1)	1.52 (−1)	...	...
60	4.92 (−1)	9.34 (−2)	1.27 (−1)	...	1.38 (−1)
70	3.08 (−1)	7.11 (−2)	9.59 (−2)	...	1.02 (−1)
80	2.05 (−1)	5.92 (−2)	8.07 (−2)	...	8.4 (−2)
90	1.45 (−1)	5.36 (−2)	7.64 (−2)	...	7.1 (−2)
100	1.07 (−1)	5.27 (−2)	7.72 (−2)	...	7.0 (−2)
110	8.35 (−2)	5.54 (−2)	8.08 (−2)	...	7.1 (−2)
120	6.76 (−2)	6.07 (−2)	...	...	7.8 (−2)
130	5.69 (−2)	6.75 (−2)	...	...	8.7 (−2)
140	4.96 (−2)	7.49 (−2)	...	...	1.11 (−1)
150	4.47 (−2)	8.17 (−2)	...	...	1.53 (−1)
160	4.15 (−2)	8.73 (−2)	...	...	...
170	3.97 (−2)	9.09 (−2)	...	...	...
180	3.92 (−2)	9.22 (−2)	...	...	...

obtained without serious difficulty from the Glauber approximation. We should note, however, that although the third-order optical potential is missing, a major part of the third Born term is included as a result of treating V_{st}, V_{abs}, and V_{pol} to *all* orders of perturbation theory.

Finally, in Tables VI and VII we present our positron results. Research activity in positron-atom scattering is in its infancy but is growing rapidly. We show in Table VI the angular distributions for positron-helium elastic scattering. It is interesting to see how radically they differ from the corresponding electron-helium elastic scattering results given in Table I, especially at small angles. The dramatic forward peaking seen in Table I is not present since now the polarization contribution is opposite in sign to that of the static potential. In fact, beginning at 300 eV one sees a slow rise, followed by a slight dip near zero degrees. In Table VII, we give the total cross sections obtained by using our values of $\mathrm{Im} f_{el}(\theta=0)$ in Eq. (3.1). The agreement between the optical-model results and the EBS results is fairly good, but the comparison with experiment shows that the optical model treatment does not lower the EBS (perturbation theory) results sufficiently.

IV. ELECTRON AND POSITRON SCATTERING FROM NEON

In Table VIII, we give a summary of our optical-model results for electron-neon elastic scattering at energies ranging from 100 to 700 eV. The Hartree-Fock orbitals of Ref. 44 were used as in helium to evaluate the various terms appearing in Eq. (2.44). An average excitation energy of 1.5 a.u. was found to give the experimental polarizability when used in Eq. (2.15), and we adopted this value for all energies in electron-neon and positron-neon scattering.

Tables IX and X compare the optical-model results at 300 and 500 eV with recent experimental values of Bromberg,[26] Jansen *et al.*,[28] and Gupta and Rees.[40] The agreement between the various experiments is quite good, with differences never much exceeding 15%. The agreement between experiment and theory is at about the same level of

TABLE X. Comparison of various theoretical and experimental differential cross sections for elastic electron–neon scattering at an incident-electron energy of 500 eV. All results are in a_0^2/sr. Numbers in parentheses are powers of 10.

θ (deg)	Theoretical values: First Born approx.	Present theory	Experimental values: Bromberg (Ref. 26)	Jansen *et al.* (Ref. 28)	Gupta and Rees (Ref. 40)
0	9.77	14.6	···	···	···
5	9.02	8.15	7.87	7.51	···
10	7.23	4.62	4.67	4.61	4.55
15	5.23	2.64	2.73	2.72	2.39
20	3.58	1.49	1.56	1.60	1.53
25	2.39	8.42 (−1)	9.13 (−1)	9.56 (−1)	9.03 (−1)
30	1.59	4.96 (−1)	5.63 (−1)	5.83 (−1)	5.80 (−1)
35	1.07	3.11 (−1)	3.57 (−1)	3.68 (−1)	3.79 (−1)
40	7.31 (−1)	2.11 (−1)	2.46 (−1)	2.47 (−1)	2.62 (−1)
45	5.11 (−1)	1.54 (−1)	1.81 (−1)	1.80 (−1)	1.80 (−1)
50	3.67 (−1)	1.19 (−1)	1.38 (−1)	1.40 (−1)	1.27 (−1)
55	2.69 (−1)	9.66 (−2)	1.11 (−1)	···	···
60	2.02 (−1)	8.05 (−2)	9.11 (−2)	···	7.9 (−2)
70	1.22 (−1)	5.95 (−2)	6.89 (−2)	···	5.9 (−2)
80	7.95 (−2)	4.69 (−2)	5.68 (−2)	···	4.8 (−2)
90	5.54 (−2)	3.93 (−2)	4.75 (−2)	···	4.2 (−2)
100	4.09 (−2)	3.49 (−2)	4.24 (−2)	···	3.8 (−2)
110	3.17 (−2)	3.25 (−2)	3.92 (−2)	···	3.3 (−2)
120	2.57 (−2)	3.14 (−2)	···	···	3.1 (−2)
130	2.16 (−2)	3.10 (−2)	···	···	3.0 (−2)
140	1.88 (−2)	3.10 (−2)	···	···	2.9 (−2)
150	1.70 (−2)	3.12 (−2)	···	···	2.9 (−2)
160	1.58 (−2)	3.15 (−2)	···	···	···
170	1.51 (−2)	3.17 (−2)	···	···	···
180	1.49 (−2)	3.17 (−2)	···	···	···

accuracy, being best at small angles. A similar situation is shown in Figs. 3–8, where we present results at 200, 400, and 700 eV. Included in these figures, in addition to the full optical-model results, are the first Born differential cross section and the static-approximation cross section obtained by approximating the optical potential simply by V_{st}. For the full optical model, it is clear that the agreement is better at small angles than at large angles. Note that the first Born approximation does very poorly at all energies.

Of particular interest is the comparison between the static results and the full optical-model results. We see that inside about 20° the lack of a polarization term and the omission of absorption effects are very serious, but at larger angles V_{st} does quite well; indeed, it typically does about as well as or occasionally better than the full optical model. A likely reason for this is that absorption and exchange tend to cancel each other at large angles and have to be handled very carefully in order to achieve excellent agreement with experiment. It is likely that the present optical-model treatment is somewhat deficient in treating the absorption potential because of our reliance on the Glauber approximation. This gives just the leading piece of the second-order absorption term in powers of k^{-1}. Thus, at zero degrees the imaginary part of our second-order amplitude with the elastic intermediate state excluded (obtained by Fourier transforming V_{abs}) will give via the optical theorem the Bethe-Born approximation to the reaction cross section, not the full Born-approximation value. In a recent study, Saxon[52] has shown that below about 500 eV the Born and Bethe-Born reaction cross sections for neon begin to differ substantially. This difficulty could in principle be avoided by the use of the full second Born term to provide the absorption potential. However, given the complexity of the Hartree-Fock orbitals in neon, this would be a very complicated task. Saxon's study of the reaction cross section shows that the full Born approximation reduces the effects of absorption below the result given by the simple Bethe-Born approximation, in the right direction to improve agreement with experiment in our work.

Another source of error is the inaccuracy inherent in the use of the Hartree-Fock wave function instead of a more-complicated correlated wave function. A simple quantity which can be used to give a rough assessment of wave-function error is $\langle 0|\mathfrak{z}^2|0\rangle$ appearing in Eq. (2.15). At small angles both Re$\bar{f}_{B2}$ and Im$\bar{f}_{B2}$ depend directly on this quantity. Using the Hartree-Fock wave function for neon one finds

$$\langle 0|\mathfrak{z}^2|0\rangle_{\mathrm{HF}} = 2.03\ ,$$

whereas an improved treatment[52] with correlation gives

$$\langle 0|\mathfrak{z}^2|0\rangle_{\mathrm{corr}} = 1.88\ ;$$

i.e., the Hartree Fock value lies nearly 10% above the more-precise correlated value. One can make approximate corrections for this effect, and when one does so, one finds changes in the elastic differential cross section which can be as large as about 10%.

Regarding exchange, the importance of a nonperturbative treatment in the case of neon is seen from the dash-dotted curve in Fig. 4, which shows the differential cross section obtained by using V^d_{opt} to approximate the optical potential, which is then treated exactly to all orders and has ex-

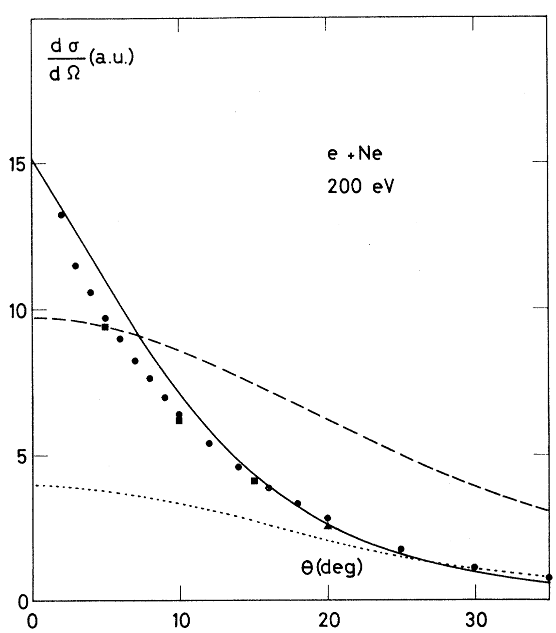

FIG. 3. Small-angle differential cross section for the elastic scattering of 200-eV electrons by neon. The solid curve is the optical-model result using Eq. (2.44) of this paper, the dashed curve is the first Born approximation, and the dotted curve is the result obtained by using only V_{st} to approximate the optical potential. The filled circles, squares, and triangles represent, respectively, the experimental results of Refs. 26, 28, and 40.

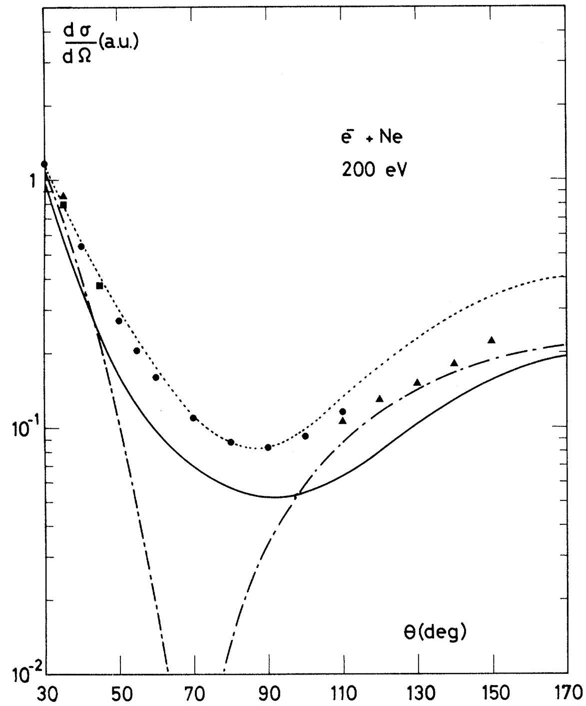

FIG. 4. Same as Fig. 3, but at large angles. We have omitted the first Born approximation since it represents the physical situation very poorly and have added a dash-dotted curve to illustrate the results obtained by using V^d_{opt} to approximate the optical potential and then adding exchange via the Ochkur approximation to the exchange amplitude.

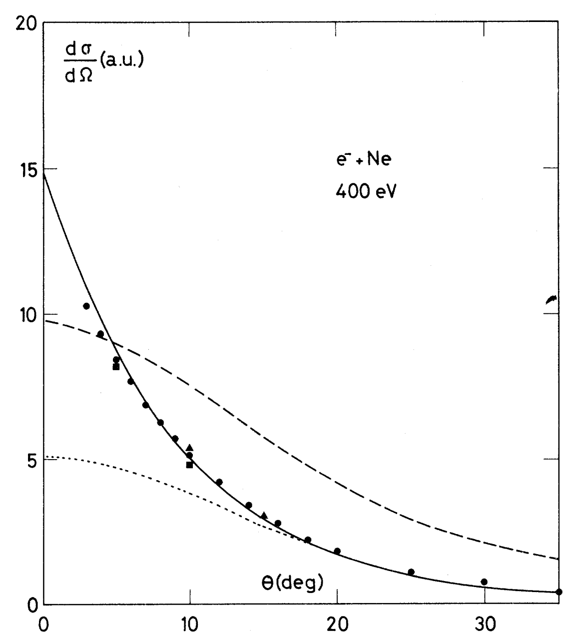

FIG. 5. Same as Fig. 3 but at 400 eV.

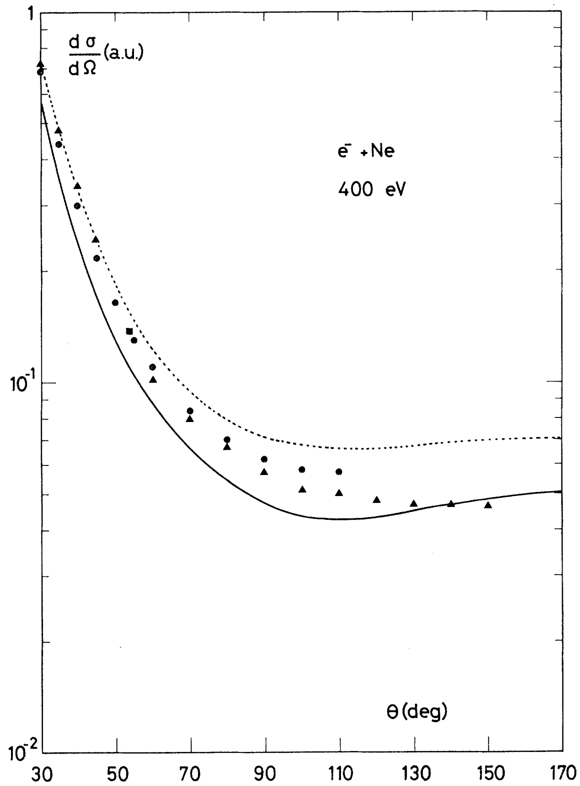

FIG. 6. Same as Fig. 5 but at large angles. Again we have omitted the first Born approximation.

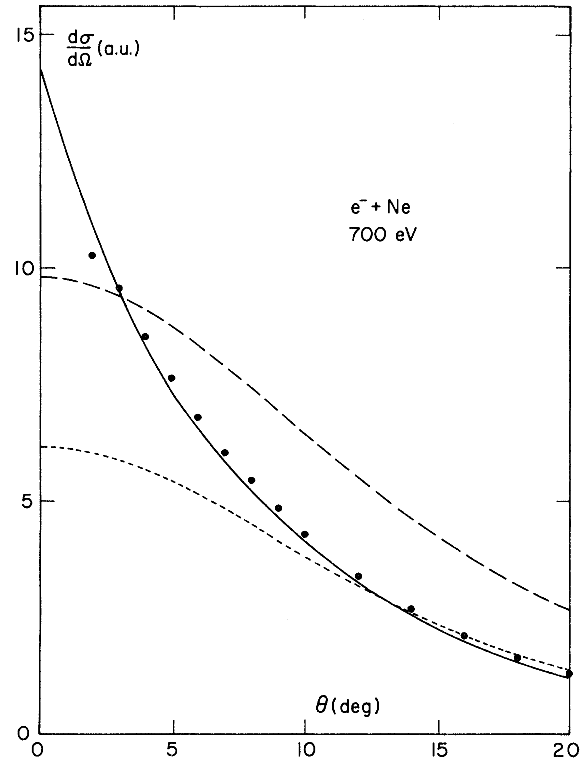

FIG. 7. Small-angle differential cross section for the elastic scattering of 700-eV electrons by neon. The solid curve is the optical-model result using Eq. (2.44) of this paper, the dashed curve is the first Born approximation, and the dotted curve is the result obtained by using only V_{st} to approximate the optical potential. The filled circles represent the experimental results of Ref. 26.

change added via the Ochkur approximation to the exchange amplitude. This treatment drastically distorts the angular distribution at angles greater than about 30°. Similar conclusions may be drawn from Table XI, which shows various approximations to the scattering amplitude. In particular, the sensitivity of the differential cross section to exchange in the vicinity of the minimum is very striking. We have found that similar results are obtained when one treats the full Mittleman-Watson exchange potential to first order in perturbation theory.

In Fig. 9 we show the various terms which contribute to V^d_{opt} at 200 eV. As one would expect, V_{st} is strongly dominant at small distances, but by the time one reaches a distance of about 2 a.u. the absorption and polarization effects begin to dominate. Finally, at about 4 a.u. the polarization term becomes the controlling factor in the optical potential, giving an asymptotic behavior

$$V^d_{opt} \simeq V_{pol} \simeq -\bar{\alpha}/2r^4. \tag{4.1}$$

The exchange pseudopotential is not shown in Fig. 9 since it falls off with increasing distance in a manner very similar to that of V_{st}. Of course, because of the factor k^{-2} in Eq. (2.43) it is smaller in magnitude than V_{st}.

Finally, Table XII shows the total cross section obtained by using $\mathrm{Im}f_{el}(\theta=0)$ in Eq. (3.1). The agreement among the various experimental values is quite good, and except at 100 eV the optical-model results are in reasonable agreement with experiment. As in helium, things begin to deteriorate badly as one goes to 100 eV, presumably reflecting the perturbative nature of our optical potential.

In terminating our discussion of electron-neon elastic scattering it is worth emphasizing the very poor quality of the first Born approximation in this intermediate-energy region. (See Figs. 3 and 5.) As discussed in I, the first Born approximation in helium is starting to be quite reasonable at an energy of 400 eV except at small momentum transfers. In fact, if one integrates the optical-

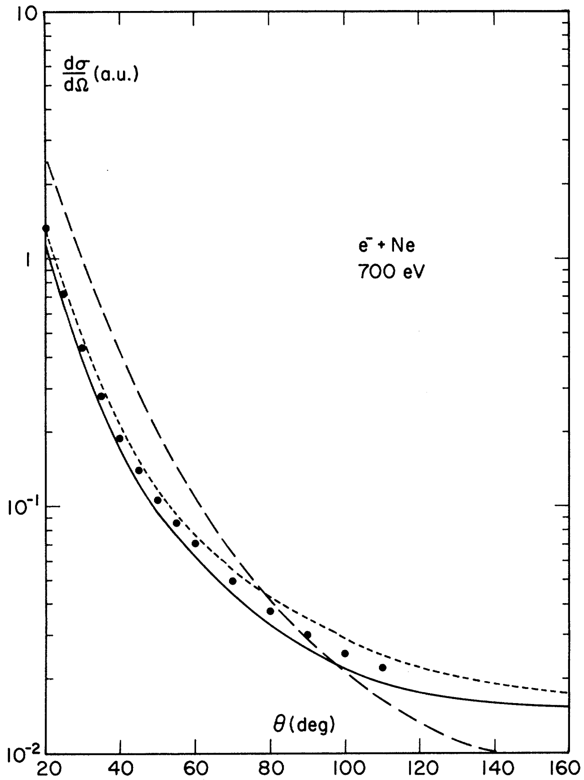

FIG. 8. Same as Fig. 7 but at large angles.

model differential cross section for electron-helium elastic scattering and compares the result with the integrated first Born differential cross section, one finds that the two differ by only 13% at 400 eV, the Born cross section being the smaller of the two. For electron-neon elastic scattering the situation is strikingly different, with the integrated Born result being a factor of 2.11 greater than the corresponding optical-model result at 400 eV.

The last two tables give our positron-neon elastic scattering results. Table XIII gives the angular distributions from 100 to 500 eV. As in the case of helium there is a slight dip at small angles above 300 eV. Table XIV summarizes our results for total cross sections and compares them with the recent experimental values of Paul.[42] The agreement between experiment and theory is seen to be satisfactory.

ACKNOWLEDGMENTS

The authors are grateful to Dr. F. J. de Heer, Dr. R. H. J. Jansen, Dr. J. P. Bromberg, Dr. J. A. Rees, and Dr. D. A. L. Paul for communicating their results prior to publication. One of us (F.W.B.) thanks the Fulbright-Hays Commission for its support while he was at the University of

TABLE XI. Comparison of various differential cross sections (in a_0^2/sr) for electron-neon scattering at 400 eV, as obtained from several approximations. Numbers in parentheses are powers of 10.

θ (deg)	First Born approx.	Opt. model with V_{st} only	Opt. model with $V^d_{opt}=V_{st}+V_{pol}$, no exchange	Opt. model with $V^d_{opt}=V_{st}+V_{pol}+iV_{abs}$, no exchange	Opt. model with $V^d_{opt}=V_{st}+V_{pol}+iV_{abs}$, Ochkur exchange	Opt. model with $V_{opt}=V_{st}+V_{pol}+iV_{abs}+V^{ex}_{opt}$
0	9.78	5.16	10.6	13.8	15.7	14.8
5	9.16	4.76	6.27	8.04	9.33	8.80
10	7.65	3.81	4.25	4.57	5.45	5.04
15	5.85	2.72	2.88	2.67	3.23	2.93
20	4.23	1.81	1.87	1.56	1.88	1.69
25	2.97	1.16	1.19	9.15 (−1)	1.07	9.76 (−1)
30	2.06	7.47 (−1)	7.61 (−1)	5.48 (−1)	6.11 (−1)	5.76 (−1)
40	1.02	3.36 (−1)	3.42 (−1)	2.24 (−1)	2.08 (−1)	2.38 (−1)
50	5.32 (−1)	1.84 (−1)	1.87 (−1)	1.18 (−1)	8.50 (−2)	1.31 (−1)
60	3.01 (−1)	1.23 (−1)	1.25 (−1)	7.71 (−2)	4.63 (−2)	8.84 (−2)
70	1.84 (−1)	9.42 (−2)	9.57 (−2)	5.85 (−2)	3.44 (−2)	6.68 (−2)
80	1.21 (−1)	7.97 (−2)	8.09 (−2)	4.88 (−2)	3.20 (−2)	5.42 (−2)
90	8.45 (−2)	7.21 (−2)	7.32 (−2)	4.34 (−2)	3.34 (−2)	4.72 (−2)
100	6.24 (−2)	6.84 (−2)	6.95 (−2)	4.04 (−2)	3.61 (−2)	4.37 (−2)
120	3.92 (−2)	6.69 (−2)	6.80 (−2)	3.79 (−2)	4.18 (−2)	4.33 (−2)
140	2.87 (−2)	6.83 (−2)	6.96 (−2)	3.75 (−2)	4.59 (−2)	4.65 (−2)
160	2.41 (−2)	7.00 (−2)	7.15 (−2)	3.76 (−2)	4.81 (−2)	4.96 (−2)
180	2.27 (−2)	7.07 (−2)	7.22 (−2)	3.77 (−2)	4.87 (−2)	5.09 (−2)

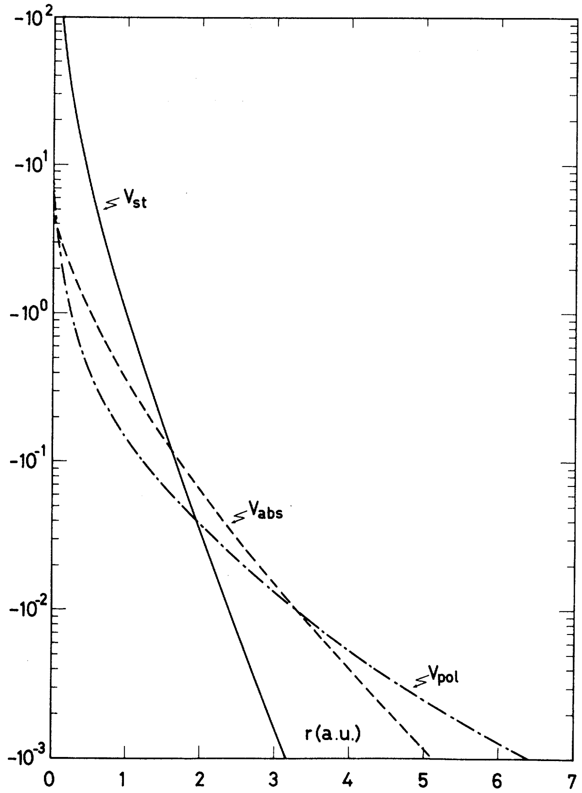

FIG. 9. Quantities V_{st}, V_{abs}, and V_{pol} as a function of the radial coordinate of the incident electron for electron-neon elastic scattering. V_{st} is independent of the electron energy; for V_{abs} and V_{pol} we have taken the energy to be 200 eV.

Brussels, where much of the work presented here was carried out.

APPENDIX

The interference between s and p orbitals can be seen clearly in Eq. (2.29) of I, which we reproduce here:

$$\bar{f}_{SB2}=\frac{2}{\pi^2}\int d\vec{q}\,\frac{1}{K_i^2K_f^2}\,\frac{1}{q^2-k'^2-i\epsilon}\times\Big[\sum_{n=1}^{Z}(\phi_n|e^{i\vec{K}\cdot\vec{r}}-e^{i\vec{K}_i\cdot\vec{r}}-e^{-i\vec{K}_f\cdot\vec{r}}+1|\phi_n)+\sum_{m,n=1}^{Z}(\phi_n|e^{i\vec{K}_i\cdot\vec{r}}-1|\phi_n)(\phi_m|e^{-i\vec{K}_f\cdot\vec{r}}-1|\phi_m)-\sum_{m,n=1}^{Z}(\phi_m|e^{i\vec{K}_i\cdot\vec{r}}-1|\phi_n)(\phi_n|e^{-i\vec{K}_f\cdot\vec{r}}-1|\phi_m)\Big], \tag{A1}$$

where $\vec{K}_i=\vec{k}_i-\vec{q}$, $\vec{K}_f=\vec{k}_f-\vec{q}$, and $k'^2=k^2-2\Delta$. The first of the three terms in the square brackets has been analyzed in I, and that analysis was the basis of the discussion in the text involving Eqs. (2.31)–(2.33). The key point is that when $\vec{K}$ becomes small (i.e., when $\vec{k}_i\simeq\vec{k}_f$) the integral on $d\vec{q}$ is nearly singular and, in fact, if one sets $\Delta=0$ so that $p_i=k_i$, the contribution to the amplitude actually diverges when $\vec{K}=0$. This situation does not obtain for the second term of Eq. (A1). Here both of the matrix elements vanish at least as rapidly as K_i^2 or K_f^2 and thus cancel the factor $K_i^{-2}K_f^{-2}$, which stands before the square brackets. There is thus no difficulty in the integration on $d\vec{q}$, even if $\Delta=0$.

However, in the third term of Eq. (A1), where m is an s state and n is a p state (or *vice versa*), the two matrix elements vary like K_i or K_f when K_i or K_f is small, so the factor $K_i^{-2}K_f^{-2}$ is not canceled. Specializing to the case when ϕ_n is a typical p orbital,

$$\phi_n(\vec{r})=\sum_j A_j r e^{-\alpha_j r}Y_{1,\mu}(\theta,\phi),$$

and ϕ_m is a typical s orbital,

$$\phi_m(r)=\frac{1}{(4\pi)^{1/2}}\sum_k B_k e^{-\beta_k r},$$

TABLE XII. Total cross sections (in units of a_0^2) for electron-neon scattering.

	Theoretical values		Experimental values		
Energy (eV)	First Born approx. (Ref. 53)	Present theory	Normand (Ref. 30)	Jansen *et al.* (Ref. 28)	de Heer and Jansen (Ref. 31)
100	29.5	14.2	9.41	10.2	11.3
200	16.8	9.64	6.96	···	7.94
300	11.9	7.53	5.38	6.1	6.44
400	9.27	6.29	4.52	···	5.49
500	7.57	5.45	···	3.6	4.77
700	5.66	4.40	···	···	···

TABLE XIII. Differential cross sections (in a_0^2/sr) for the elastic scattering of positrons by neon in the energy range 100–500 eV, as obtained from the present *ab initio* optical-model theory. Numbers in parentheses are powers of 10.

θ (deg)	Energy (eV) 100	200	300	400	500
0	3.78	4.24	4.60	4.89	5.14
2	3.50	4.13	4.65	5.07	5.42
5	3.10	3.75	4.23	4.56	4.78
10	2.44	2.89	3.10	3.18	3.21
15	1.85	2.06	2.08	2.03	1.95
20	1.37	1.41	1.33	1.24	1.14
25	1.00	9.42 (−1)	8.38 (−1)	7.43 (−1)	6.60 (−1)
30	7.23 (−1)	6.21 (−1)	5.26 (−1)	4.51 (−1)	3.93 (−1)
35	5.15 (−1)	4.09 (−1)	3.36 (−1)	2.84 (−1)	2.45 (−1)
40	3.65 (−1)	2.74 (−1)	2.23 (−1)	1.88 (−1)	1.62 (−1)
50	1.83 (−1)	1.35 (−1)	1.12 (−1)	9.51 (−2)	8.16 (−2)
60	9.69 (−2)	7.76 (−2)	6.59 (−2)	5.59 (−2)	4.76 (−2)
70	5.73 (−2)	5.09 (−2)	4.31 (−2)	3.61 (−2)	3.03 (−2)
80	3.87 (−2)	3.62 (−2)	3.02 (−2)	2.49 (−2)	2.07 (−2)
90	2.92 (−2)	2.72 (−2)	2.23 (−2)	1.81 (−2)	1.49 (−2)
120	1.67 (−2)	1.44 (−2)	1.13 (−2)	8.95 (−3)	7.21 (−3)
150	1.20 (−2)	1.00 (−2)	7.74 (−3)	6.05 (−3)	4.83 (−3)
180	1.08 (−2)	8.89 (−3)	6.84 (−3)	5.33 (−3)	4.24 (−3)

one readily finds for the corresponding contribution to the third term of Eq. (A1) (setting $\gamma_{jk} = \alpha_j + \beta_k$ and $\gamma_{st} = \alpha_s + \beta_t$)

$$\frac{192}{\pi^2} \sum_{j,k,s,t} A_j B_k A_s B_t \times \int d\vec{q} \frac{1}{q^2 - k'^2 - i\epsilon} \times \frac{1}{K_i^2 K_f^2} \frac{K_i^2 + K_f^2 - K^2}{(K_i^2 + \gamma_{jk}^2)^3 (K_f^2 + \gamma_{st}^2)^3}. \tag{A2}$$

Since one wants only the part of this expression which is singular at $K=0$ as $\Delta \to 0$, one merely decomposes whenever necessary products like $K_i^{-2}(K_i^2 + a^2)^{-1}$ via partial fractions. All the singular integrals can thus be brought to a form where Eqs. (2.38b) and (2.39b) of I can be employed. In this fashion the singular part of Eq. (A2) can be reduced to

$$\frac{2}{k} |\langle m|z|n\rangle|^2 \left(\ln\frac{2}{\delta} - \frac{K}{(K^2+\delta^2)^{1/2}} \ln\frac{K + (K^2+\delta^2)^{1/2}}{\delta} \right) \tag{A3}$$

through leading order in k^{-1}. Subtracting the $\delta \to 0$ ($\Delta \to 0$) limit from this expression one finds

$$\frac{2}{k} |\langle m|z|n\rangle|^2 \left(\ln K + \ln\frac{2}{\delta} - \frac{K}{(K^2+\delta^2)^{1/2}} \ln\frac{K + (K^2+\delta^2)^{1/2}}{\delta} \right). \tag{A4}$$

It is this expression, multiplied by 4 (two spins, two orderings of m and n), which must be added to f_{corr} of Eq. (2.33) to give the full V_{corr} when used in Eq. (2.35).

The great similarity between Eq. (A4) and Eq.

TABLE XIV. Total cross sections (in units of a_0^2) for positron-neon scattering.

Energy (eV)	Theoretical values: First Born approx. (Ref. 53)	Theoretical values: Present theory	Experimental values: Paul (Ref. 42)
100	29.5	8.42	6.4
200	16.8	6.74	5.5
300	11.9	5.68	4.6
400	9.27	4.95	⋯
500	7.57	4.41	⋯

(2.33) should be noted. Since the expression of Eq. (A4) falls off only like $k^{-3}K^{-2}$ as $K\to\infty$, we have in practice cut it off at large K in the same fashion as in Eq. (2.33), i.e., by a factor which is 1 when K is much less than the inverse of a typical atomic size and which falls off rapidly for large K. This is clearly called for, since an inspection of Eq. (A1) shows that the expression under consideration actually falls off quite rapidly as $K\to\infty$.

---

*Research supported in part by the NATO Scientific Affairs Division under Grant No. 586.

[1]F. W. Byron, Jr. and C. J. Joachain, Phys. Rev. A 8, 1267 (1973). This paper will be referred to as I.
[2]F. W. Byron, Jr. and C. J. Joachain, Phys. Rev. A 8, 3266 (1973).
[3]F. W. Byron, Jr. and C. J. Joachain, J. Phys. B 7, L212 (1974).
[4]M. H. Mittleman and K. M. Watson, Phys. Rev. 113, 198 (1959).
[5]M. H. Mittleman and K. M. Watson, Ann. Phys. (N.Y.) 10, 268 (1960).
[6]M. L. Goldberger and K. M. Watson, *Collision Theory* (Wiley, New York, 1964), Chap. 11.
[7]C. J. Joachain, *Quantum Collision Theory* (North-Holland, Amsterdam, 1975), Chap. 20.
[8]R. T. Pu and E. Chang, Phys. Rev. 151, 31 (1966).
[9]H. P. Kelly, Phys. Rev. 160, 44 (1967); 166, 47 (1968); 171, 54 (1968).
[10]R. W. LaBahn and J. Callaway, Phys. Rev. 180, 91 (1969); 188, 520 (1969).
[11]J. E. Purcell, R. A. Berg, and A. E. S. Green, Phys. Rev. A 2, 107 (1970); P. S. Ganas, S. K. Dutta, and A. E. S. Green, Phys. Rev. A 2, 111 (1970).
[12]M. H. Mittleman, Phys. Rev. A 2, 1846 (1970).
[13]C. J. Joachain and M. H. Mittleman, Phys. Lett. 36A, 209 (1971).
[14]C. J. Joachain and M. H. Mittleman, Phys. Rev. A 4, 1492 (1971).
[15]S. P. Khare and P. Shobha, J. Phys. B 4, 208 (1971).
[16]J. B. Furness and I. E. McCarthy, J. Phys. B 6, 2280 (1973).
[17]S. P. Khare and P. Shobha, J. Phys. B 7, 420 (1974).
[18]F. W. Byron, Jr. and C. J. Joachain, Phys. Rev. A 9, 2559 (1974). This paper will be referred to as II.
[19]F. W. Byron, Jr. and C. J. Joachain, Phys. Lett. 49A, 306 (1974).
[20]F. W. Byron, Jr. and C. J. Joachain, in *Electron and Photon Interactions with Atoms*, edited by H. Kleinpoppen and M. R. C. McDowell (Plenum, New York and London, 1976), p. 299.
[21]C. J. Joachain and C. Quigg, Rev. Mod. Phys. 46, 279 (1974).
[22]We emphasize that in choosing the average excitation energy Δ in this manner we are *not* fitting our theory to any experimental data.
[23]J. P. Bromberg, J. Chem. Phys. 50, 3906 (1969).
[24]G. B. Crooks and M. E. Rudd, Bull. Am. Phys. Soc. 17, 131 (1971); G. B. Crooks, thesis (University of Nebraska, 1972) (unpublished).
[25]N. Oda, F. Nishimura, and S. Tahira, J. Phys. Soc. Jpn. 33, 462 (1972).
[26]J. P. Bromberg, J. Chem. Phys. 61, 963 (1974), and private communication.
[27]S. K. Sethuraman, J. A. Rees, and J. R. Gibson, J. Phys. B 7, 1741 (1974).
[28]R. H. J. Jansen, F. J. de Heer, H. J. Luyken, B. van Wingerden, and H. J. Blaauw, J. Phys. B (to be published); R. H. J. Jansen, thesis (University of Amsterdam, 1975) (unpublished).
[29]R. B. Brode, Phys. Rev. 25, 636 (1925).
[30]C. E. Normand, Phys. Rev. 35, 1217 (1930).
[31]F. J. de Heer and R. H. J. Jansen, FOM Instituut voor Atoom-en Molecuulfysica, Amsterdam, Report No. 37173, 1975 (unpublished); J. Phys. B (to be published).
[32]K. F. Canter, P. G. Coleman T. C. Griffith, and G. R. Heyland, J. Phys. B 6, L201 (1973).
[33]P. G. Coleman, T. C. Griffith, G. R. Heyland, and T. L. Killeen, in Ref. 20.
[34]B. Jaduszliwer, A. Nakashima, and D. A. L. Paul, Can. J. Phys. 53, 962 (1975).
[35]J. Dutton, F. M. Harris, and R. A. Jones, J. Phys. B 8, L65 (1975), and private communication.
[36]E. M. A. Peixoto, C. F. Bunge, and R. A. Bonham, Phys. Rev. 181, 322 (1969).
[37]M. Fink and A. C. Yates, At. Data 1, 385 (1970).
[38]D. G. Thompson, J. Phys. B 4, 468 (1971).
[39]D. W. Walker, quoted in Ref. 40.
[40]S. C. Gupta and J. A. Rees, J. Phys. B 8, 417 (1975).
[41]F. J. de Heer and R. H. J. Jansen, FOM Instituut voor Atoom-en Molecuulfysica, Amsterdam, Report No. 37174, 1975 (unpublished); J. Phys. B (to be published).
[42]D. A. L. Paul (private communication).
[43]F. W. Byron, Jr., C. J. Joachain, and E. H. Mund, Phys. Rev. D 8, 2622 (1973); 11, 1662 (1975).
[44]E. Clementi, Tables of Atomic Functions, San Jose Research Laboratory, I.B.M., San Jose, Calif., 1965 (unpublished).
[45]W. M. Huo, J. Chem. Phys. 56, 3468 (1972); 57, 4800 (1972).
[46]R. J. Glauber, in *Lectures in Theoretical Physics*, edited by W. E. Brittin (Interscience, New York, 1959), Vol. 1, p. 315.
[47]Although this result is not given explicitly in Ref. 14, it is a straightforward matter to derive it from Eqs. (3.15)–(3.19) of that paper.
[48]A. C. Yates, Chem. Phys. Lett. 25, 480 (1974).
[49]By this we mean that for large r the terms in question vary like a polynomial in r times e^{-Z^*r}.
[50]M. Inokuti, Y. K. Kim, and R. L. Platzman, Phys. Rev. 164, 55 (1967).
[51]That is, the sum of the Bethe-Born total reaction (nonelastic) cross section of Ref. 50 and of the first Born total elastic cross section.
[52]R. P. Saxon, Phys. Rev. A 8, 839 (1973).
[53]M. Inokuti and M. R. C. McDowell, J. Phys. B 7, 2382 (1974).